LA-UR-97-2162

Title:

Extracting the Equation of State of Nuclear Matter through Hydrodynamical Analysis

Author(s): B.R. Schlei

Submitted to:

LA-UR-97-2162

Extracting the Equation of State of Nuclear Matter through Hydrodynamical Analysis

B.R. Schlei[1,a]

[1] Theoretical Division, Los Alamos National Laboratory,
Los Alamos, NM 87545, USA

June 6, 1997

Abstract. Predominantly preliminary single and double inclusive momentum spectra of 158 $AGeV$ Pb+Pb collisions, recently measured by the NA44 and NA49 Collaborations, are reproduced using the relativistic hydrodynamical model HYLANDER-C. Two different equations of state, which both contain a phase transition to a quark-gluon plasma, can be used to reproduce the (preliminary) data. The space-time geometries in the two calculations differ strongly. However, the Bose-Einstein correlation functions of identical pion pairs do not show such a strong, but still a significant sensitivity to the effects of the equations of state.

1. Introduction

Fluid dynamics provides an intuitively simple description of heavy-ion collisions: two nuclei smash into each other and are rapidly thermalized and compressed; the resulting zone of very hot and dense nuclear matter (the so-called fireball) then expands and breaks up into bits of hadronic matter that ultimately reach the detectors. In a 158 $AGeV$ Pb+Pb reaction the velocity of the incoming projectile is 0.99998 c; since the sound speed in the ground state of nuclear matter is about $\sim$ 0.2 c, shock waves are formed. The density achieved in the center of the hot fireball is calculated to be as much as 20 times that of normal nuclear matter. Under such extreme conditions, a quark-gluon plasma (QGP) can be formed, which in our calculations can reach an appreciable fraction of the total matter [1],[2].

Many experimental observables have been suggested with which one might ascertain whether a quark-gluon plasma (QGP) has been formed in relativistic heavy-ion collisions, or with which one can obtain some idea of the evolution of the experimentally generated fireballs. By measuring the correlations of identical particles (Bose-Einstein correlations (BEC)), one can get a measure of the sizes and lifetimes of the fireballs [3]. This is very similar to the concept behind the Hanbury-Brown/Twiss effect used to measure the size of stars [4].

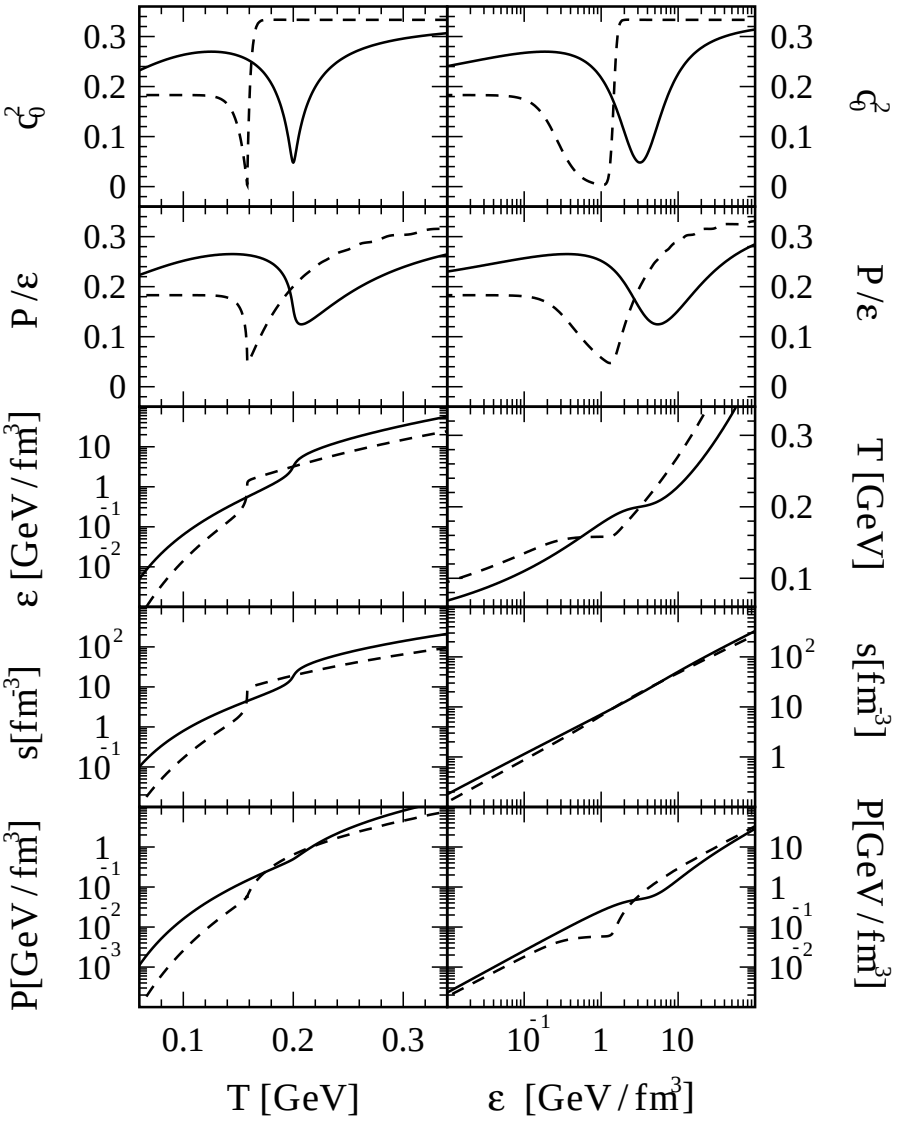

Fig. 1. Pressure, P, entropy density, s, energy density, ϵ, ratio of pressure and energy density, P/ϵ, speed of sound, c_0^2, and temperature, T, as functions of T and/or ϵ, for the equations of state EOS-I (solid lines) and EOS-II (dashed lines), respectively (see text).

It is the purpose of this paper to use in a hydrodynamical analysis two not too different equations of state (EOS) in the attempt to reproduce the predominantly preliminary single inclusive momentum spectra of 158 $AGeV$ Pb+Pb collisions, recently measured by the NA44 [5],[6] and NA49 Collaborations [7], and to learn which details of the calculations are most sensitive to the effects of the EOS. We shall also learn about the initial conditions which one has to use while considering the chosen equations of state. After a comparison of the theoretical calculations with the measurements, we exhibit the space-time geometries of the real hadron sources in the two scenarios, and discuss their particular features. Finally, we shall calculate inverse width parameters of Bose-Einstein correlation functions of identical pion pairs for the two different hydrodynamical solutions and compare the results to preliminary BEC data taken by the NA49 Collaboration [8].

2. The Model, the Equations of State, and the Initial Conditions

2.1. The Model

Among the large number of models (*cf.* refs. [2],[9] and refs. therein) which apply relativistic hydrodynamics to relativistic heavy-ion collisions, we choose for the following to use the model[b] HYLANDER-C.

This model applies 3+1-dimensional relativistic one-fluid-dynamics, and provides fully three-dimensional solutions of the hydrodynamical relativistic Euler-equations [13]. One has to specify an equation of state, initial distributions, e.g., in form of parameterizations with initial parameters (*cf.*, refs. [2],[11]), and a break-up (freeze-out) condition in order to obtain an unambiguous solution from the hydrodynamical equations. In the calculations we shall assume that hadronization occurs for all particle species at the same fixed freeze-out temperature $T_f = 139\ MeV$.

All model calculations are based on the assumption of thermal as well as on chemical equilibrium. In both types of spectra (single inclusive momentum spectra and BEC, respectively) we shall include resonance decays. In particular, the momentum distributions are calculated in terms of the generalized Cooper-Frye formula (see ref. [14]), where explicitly a baryon and a strangeness chemical potential are taken into account [11]. The subsequent calculations of Bose-Einstein correlations are performed using the formalism outlined in ref. [15]. The hadron source is assumed to be fully chaotic; the influence of partial coherence [15] will not be considered here.

2.2. The Equations of State

Any type of EOS can be considered when solving the relativistic Euler-equations. In Fig. 1 the two equations of state, which we are going to use in the following, are plotted in many different representations.

The first equation of state, EOS-I, has been used in many recent calculations

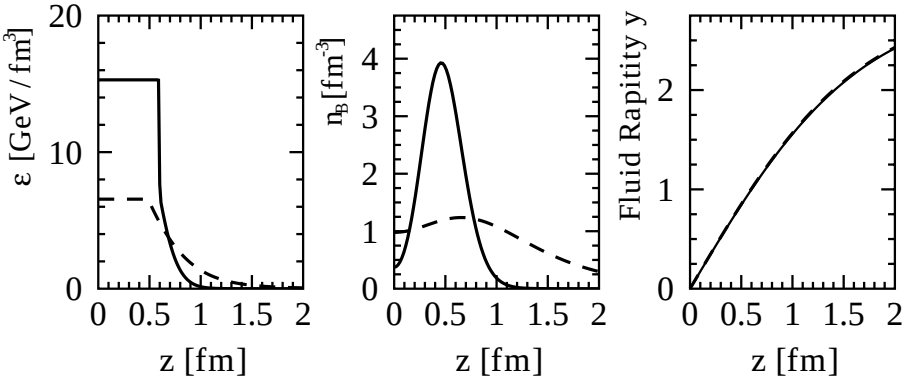

Fig. 2. Initial distributions of the energy density, ϵ, the baryon density, n_B, and the fluid rapidity, y, plotted against the longitudinal coordinate z. The solid lines indicate the initial distributions for the use with EOS-I, whereas the dashed lines indicate the initial distributions for the use with EOS-II, respectively.

(*cf.*, e.g. refs. [1],[2],[11],[15]), in the successful attempt to reproduce hadronic single inclusive momentum spectra and BEC, which have been measured in relativistic heavy-ion collision experiments. In particular, EOS-I exhibits a phase transition to a quark-gluon plasma at a critical temperature $T_c = 200\ MeV$ with a critical energy density $\epsilon_c = 3.2\ GeV/fm^3$ (*cf.*, refs. [16],[17],[18]).

The second equation of state, EOS-II, is also a lattice QCD based EOS which has recently become very popular in the field of relativistic heavy-ion physics (*cf.*, ref. [19]). This equation of state includes a phase transition to a quark-qluon plasma at $T_c = 160\ MeV$ with a critical energy density $\epsilon_c \approx 1.5\ GeV/fm^3$.

Both EOS have no dependence on the baryon density. For instance, in Fig. 1 the plot of $P(\epsilon)/\epsilon$ emphasizes the existence of a minimum P/ϵ at $\epsilon = \epsilon_c = 3.2\ GeV/fm^3$ ($\approx 1.5\ GeV/fm^3$) for EOS-I (EOS-II), referred to as *the softest point* of the EOS. It corresponds to the boundary between the generalized mixed phase and the QGP [19]. As it can be seen in Fig. 1, EOS-II yields a much softer equation of state than EOS-I.

2.3. The Initial Conditions

In the following it is assumed that due to an experimental uncertainty for the centrality of the collision, only 90% of the total available energy and the total baryon number have been observed. It is then possible to find initial distributions for the two here considered equations of state, such that one can reproduce the (preliminary) single inclusive momentum spectra of 158 $AGeV$ Pb+Pb collisions, which have been measured recently by the NA44 and NA49 Collaborations.

Fig. 2 shows the initial distributions for the energy density, $\epsilon(z)$, the baryon

density, $n_B(z)$, and the fluid rapidity, $y(z)$, plotted against the longitudinal coordinate z. We use here for the initial distributions the initial condition scenarios which have been extensively described in refs. [2] and [11]. In particular, it is assumed that an initial transverse fluid velocity field is completely absent, and the initial longitudinal distributions for energy density, ϵ, and baryon density, n_B, are smeared out with a Woods-Saxon parametrization in the transverse direction, $r_\perp$ (*cf.*, ref. [15]). The choices for the initial parameters, which in each case provide the best fit results for the hadronic single inclusive momentum spectra of the two considered experiments, are in case of EOS-I (EOS-II): relative fraction of thermal energy in the central fireball, $K_L = 0.55$ (0.20), longitudinal extension of the central fireball, $\Delta = 1.20\ fm$ (1.00 fm), rapidity at the edge of the central fireball, $y_\Delta =$ 1.00 (0.85), rapidity at maximum of initial baryon y distribution, $y_m = 0.80$ (1.50), and width of initial baryon y distribution, $\sigma = 0.32$ (1.00), respectively.

The maximum initial energy density is $\epsilon_\Delta = 15.3\ GeV/fm^3$ (6.55 GeV/fm^3), and the maximum initial baryon density is $n_B^{max} = 3.93\ fm^{-3}$ (1.24 fm^{-3}), for EOS-I (EOS-II), respectively. 71% (30%) of the baryonic matter is initially located in the central fireball region. Hence, the use of EOS-I predicts a much larger stopping than the use of EOS-II.

It should be stressed here, that it is really neccessary to use such extremely different initial conditions for EOS-I and EOS-II. If one just uses different equations of state without changing the initial conditions, which in fact are unknown for 158 $AGeV$ Pb+Pb collisions, one would have obtained single inclusive momentum spectra which differ by up to 20% - 30% when comparing the calculations for EOS-I and EOS-II.

3. Single Inclusive Momentum Spectra

Figs. 3 - 6 show the results of the hydrodynamical calculations compared to the preliminary and final single inclusive momentum spectra of the 158 $AGeV$ Pb+Pb collisions, which have been measured by the NA44 [5],[6] and NA49 Collaborations [7]. All single inclusive momentum spectra have been evaluated in the nucleus-nucleus center of mass system ($y_{cm} = 2.91$).

In case of EOS-I (EOS-II) the average value for the baryonic chemical potential is $\langle \mu_B \rangle = 324\ MeV$ (360 MeV), and the average value for the strangeness chemical potential is $\langle \mu_S \rangle = 55\ MeV$ (69 MeV), using $T_f = 139\ MeV$ for the freeze-out temperature. The energy density at freeze-out is $\epsilon_f = 0.292\ GeV/fm^3$ (0.126 GeV/fm^3). Both calculations yield considerably good agreement with both experiments. However, the calculations for the much softer EOS-II already gives larger slopes in the transverse mass spectra compared to the calculations for EOS-I. The different slopes in the transverse mass spectra have their origin in the different transverse velocity fields at freeze-out. For EOS-I we obtain a maximum transverse velocity $v_\perp^{max}(I) = 0.46\ c$, whereas for EOS-II we get the much smaller value $v_\perp^{max}(II) = 0.30\ c$.

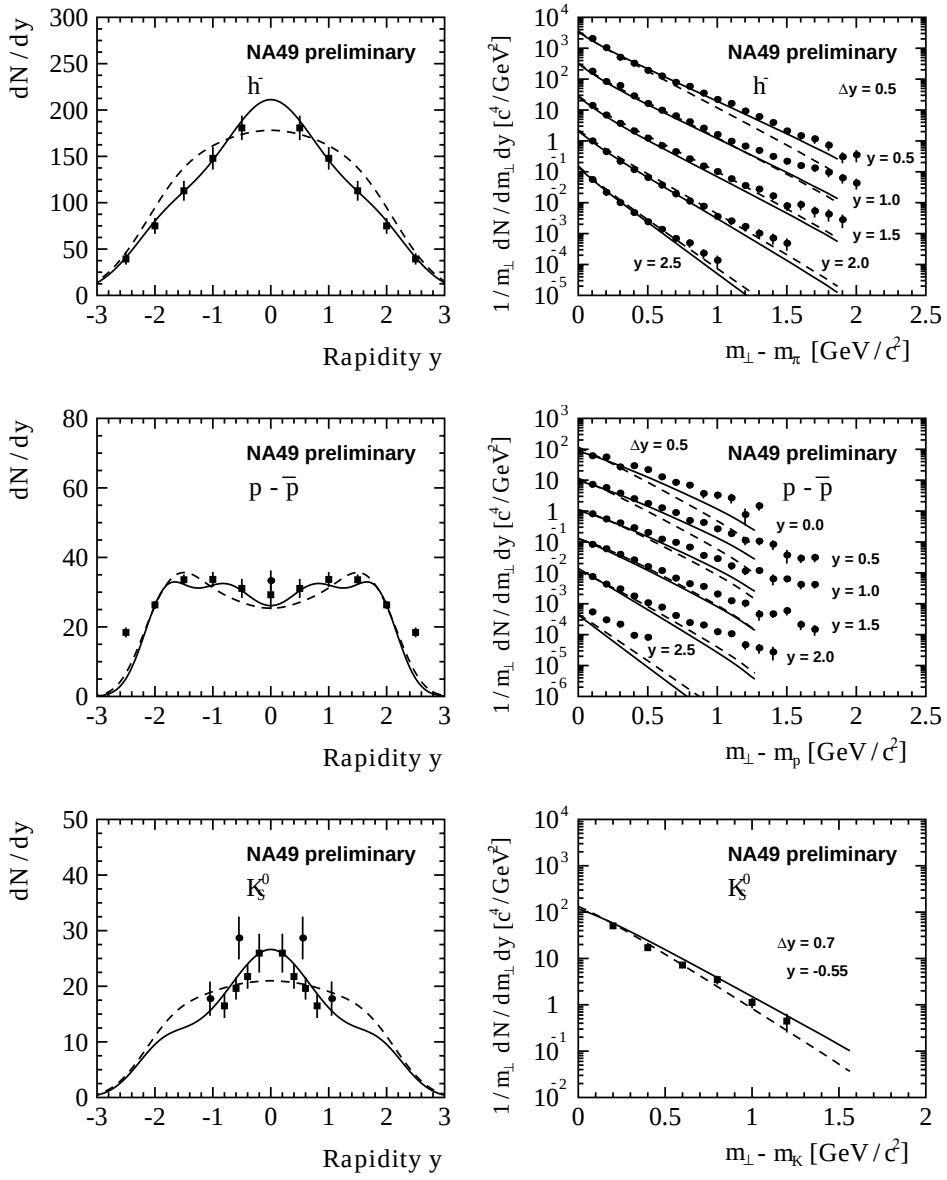

Fig. 3. Rapidity spectra, dN/dy, and transverse mass spectra, $1/m_\perp dN/dm_\perp$, for negative hadrons, h^- (*i.e.*, π^-, K^-, $\bar{p}$), net protons (without contributions from Λ^0 decay), $p-\bar{p}$, and neutral kaons, K^0_S, respectively. The solid lines indicate the results of the calculations when using equation of state EOS-I, whereas the dashed lines represent the results when using equation of state EOS-II. The shown preliminary data have been taken by the NA49 Collaboration [7].

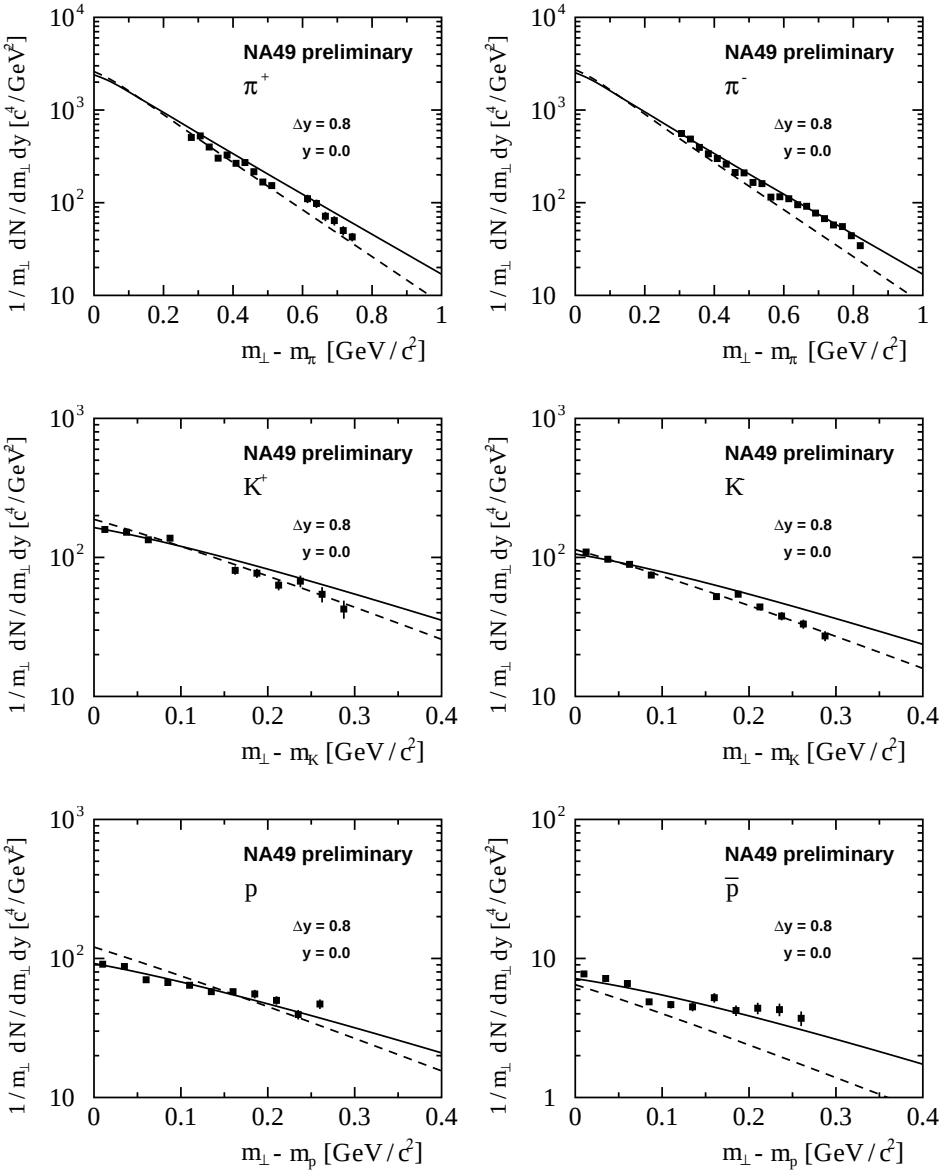

Fig. 4. Transverse mass spectra, $1/m_\perp dN/dm_\perp$, for pions, π^+ and π^-, kaons, K^+ and K^-, protons (without contributions from Λ^0 decay), p, and anti-protons, $\bar{p}$, respectively. The solid lines indicate the results of the calculations when using equation of state EOS-I, whereas the dashed lines represent the results when using equation of state EOS-II. The shown preliminary data have been taken by the NA49 Collaboration [7].

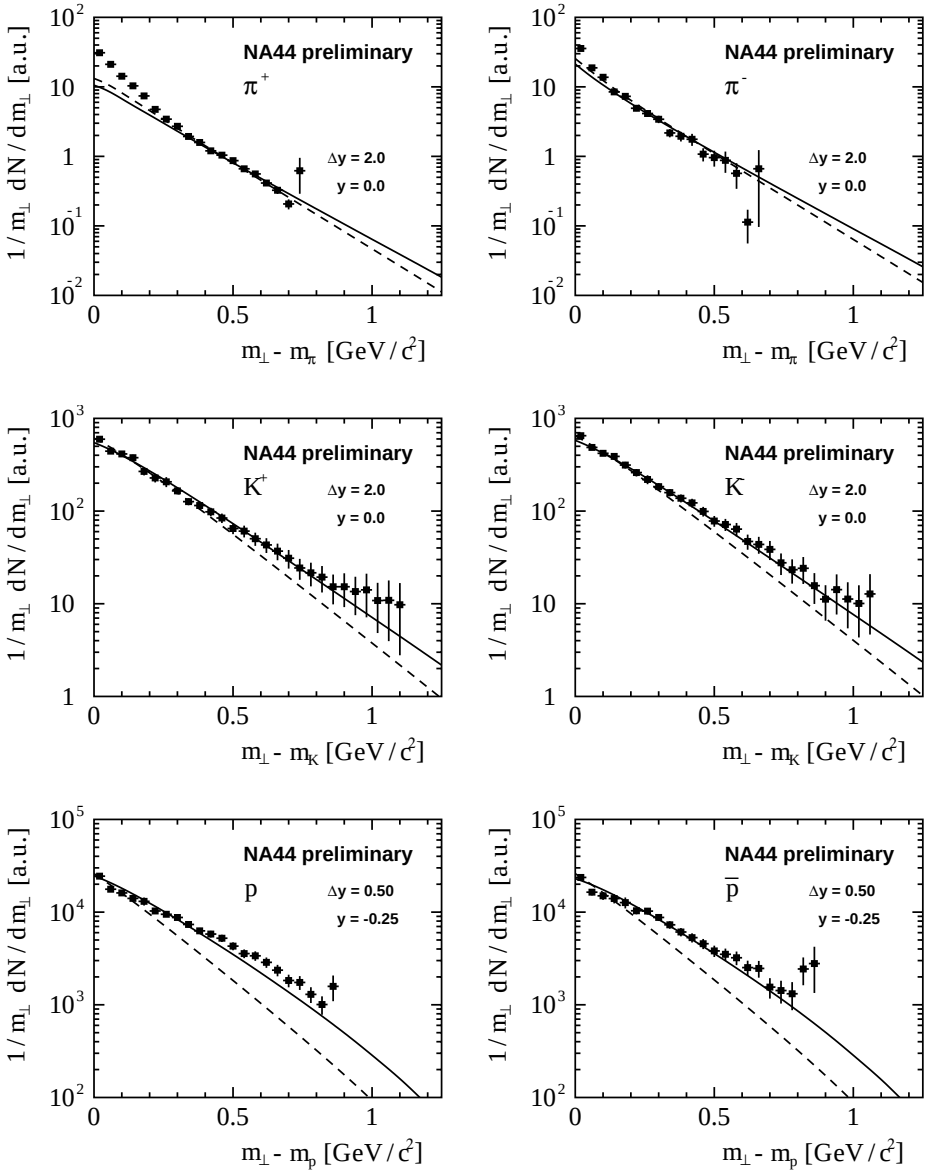

Fig. 5. Unnormalized transverse mass spectra, $1/m_\perp dN/dm_\perp$, for pions, π^+ and π^-, kaons, K^+ and K^-, protons (including contributions from Λ^0 decay), p, and anti-protons, $\bar{p}$, respectively. The solid lines indicate the results of the calculations when using equation of state EOS-I, whereas the dashed lines represent the results when using equation of state EOS-II. The shown preliminary data have been taken by the NA44 Collaboration [5].

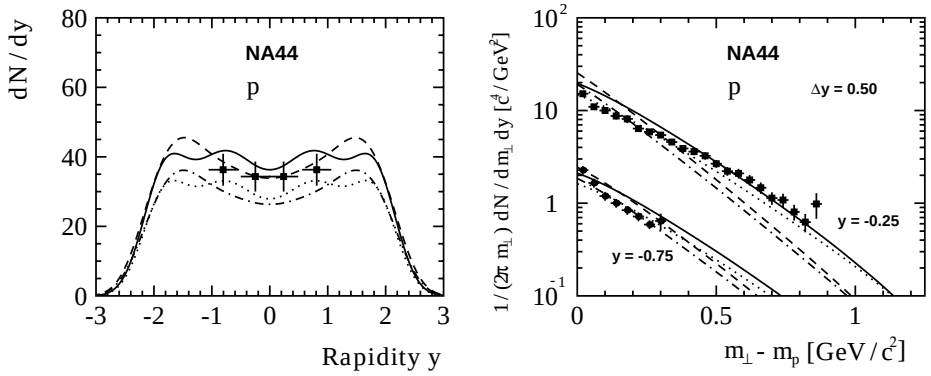

Fig. 6. Rapidity spectra, dN/dy, and transverse mass spectra, $1/m_\perp dN/dm_\perp$, for protons, p, respectively. The solid (dotted) lines indicate the results of the calculations when using equation of state EOS-I including (without) contributions from Λ^0 decay, whereas the dashed (dashed-dotted) lines represent the results when using equation of state EOS-II including (without) contributions from Λ^0 decay. The data have been taken by the NA44 Collaboration [6].

Since the data analysis for the 158 $AGeV$ Pb+Pb collisions has not been finished yet by the NA44 and NA49 Collaborations, we cannot draw too many conclusions here. Therefore, in the following we shall look into the space-time features of the hydrodynamical model calculations and try to learn, whether Bose-Einstein correlations provide a more distinct observable in the attempt to decide which one of the two considered EOS gives a better description of the data.

4. Space-Time Geometry and Bose-Einstein Correlations

In Fig. 7 it can be seen, that the hydrodynamical solutions which are provided from the numerical analysis represent an evolution of initally disk-shaped fireballs which emit hadrons from the very beginning of their formation. While the relativistic fluids expand in longitudinal and in transverse directions, the longitudinal positions of the freeze-out points increase their distance relative to the center. Because of the effect of transverse inwardly moving rarefaction waves, the transverse freeze-out positions move towards the center of the fireball. In the late stage of the hydrodynamic expansion the hadron-emitting fireballs separate into two parts while cooling down until they cease to emit.

For both equations of state we obtain fireballs which have similar transverse sizes and a QGP phase of similar lifetime. For EOS-I (EOS-II) the total lifetime of the QGP is $t_{QGP} = 2.4\ fm/c$ (3.0 fm/c), considering the critical temperature T_c = 200 MeV (160 MeV). However, the softer EOS-II results in a fireball that has a much larger longitudinal size than the fireball which is governed by EOS-I. The total lifetime of the fireball is $t_{max} = 29.3\ fm/c$ (13.1 fm/c) for EOS-II (EOS-I).

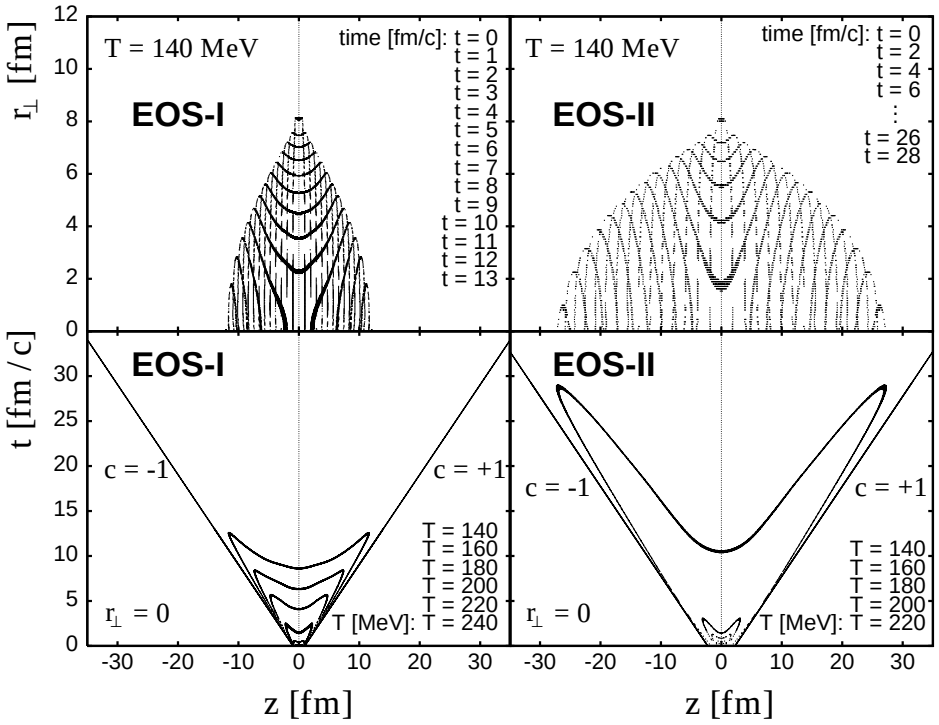

Fig. 7. Time contour plots of the freeze-out hypersurfaces in the $z - r_\perp$ plane, and temperature evolution plots at $r_\perp = 0$, for the relativistic fluids governed by EOS-I and EOS-II, respectively. In the time contour plots, each line represents an isotherme ($T_f = 140\ MeV$) at a fixed time t (timesteps $\Delta t = 1.0\ fm/c$). In the temperature evolution plots, each line corresponds to a fixed temperature, T (temperature steps $\Delta T = 20\ MeV$).

Such large differences (factor ~ 2) in the lifetimes and longitudinal sizes of the two considered scenarios should show up in the inverse widths of the transverse "out" [20] and longitudinal Bose-Einstein correlations of identical pion pairs.

In Fig. 8 inverse widths of BEC functions of identical negative pion pairs (including decay contributions from resonances) are shown, which have been extracted with a Gaussian fit as explained in refs. [21],[22], in comparison with preliminary measurements of the NA49 Collaboration [8]. The inverse widths are plotted as functions of the average transverse momentum of the pion pair, $K_\perp$. The effective longitudinal radii, R_{long}, are evaluated in the longitudinal comoving system (LCMS), whereas all other effective transverse radii, R_{side} and R_{out}, have been calculated in the nucleus-nucleus center of mass system. Since BEC of negative pions are in general not of Gaussian shape, (*cf.*, e.g., refs. [1],[15],[23]), the fit to a Gaussian generates an error for the inverse width parameters.

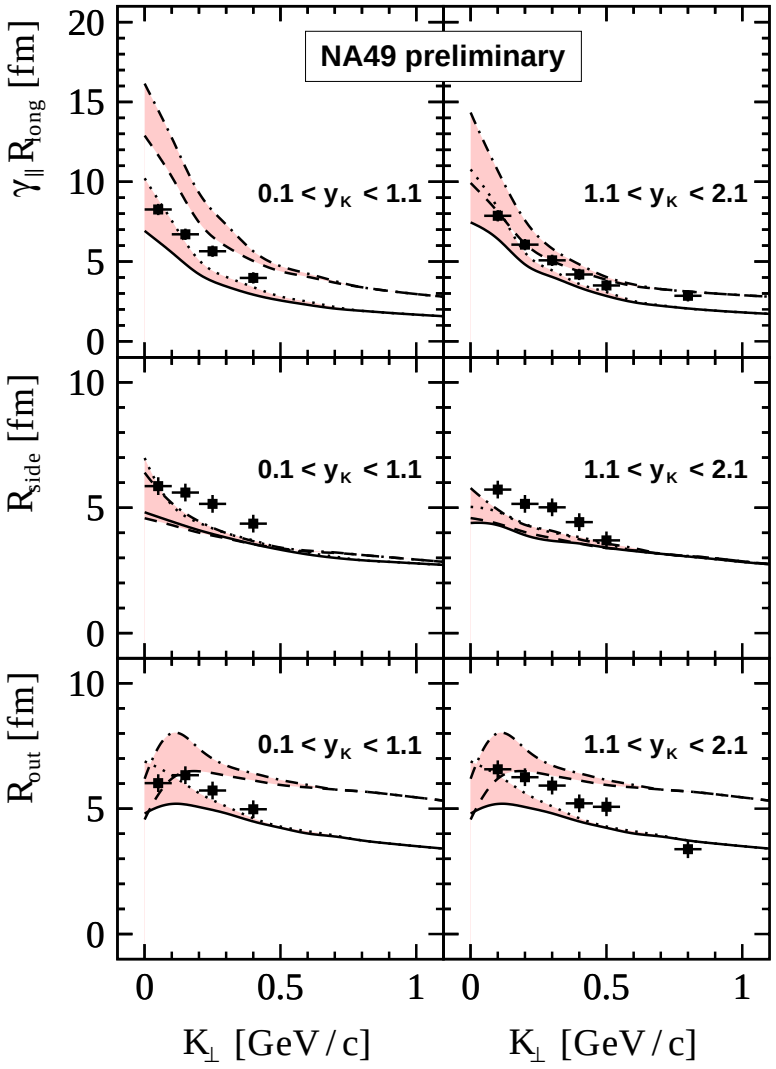

Fig. 8. Inverse widths of BEC functions of identical negative pion pairs (including decay contributions from resonances) as functions of the average transverse momentum of the boson pair, $K_\perp$, in the indicated ranges of the particle pair rapidities, y_K, compared to preliminary data of the NA49 Collaboration [8], respectively. The solid (dashed) lines indicate the inverse widths of BEC functions extracted from a Gaussian fit for the calculation using EOS-I (EOS-II). The dotted (dashed-dotted) lines are the true inverse widths of the correlation functions at their 68% level (see text), and the grey zones reflect the theoretical uncertainties, when extracting the inverse widths.

Therefore, in Fig. 8 also the true inverse widths of the correlation functions are included at their 68% level, i.e., the inverse widths at $0.68 \cdot (I_0 - 1)$, where $I_0 \equiv C_2(\vec{k}, \vec{k})$ is the intercept of the BEC function, $C_2(\vec{k}_1, \vec{k}_2)$, of two identical pions with momenta $\vec{k}_1$ and $\vec{k}_2$, respectively.

As expected, the transverse radii R_{side} as functions of $K_\perp$ are very similar when comparing the calculations for EOS-I with the calculations for EOS-II. The transverse radii R_{out} and the longitudinal radii R_{long} are larger for the calculation using EOS-II compared to the calculation using EOS-I. But the differences, e.g., in the longitudinal effective radii are not so pronounced anymore as in the case of the longitudinal sizes of the exhibited space-time geometries of the hadron sources. However, they are quite significant.

Unfortunately, the data analysis of the Bose-Einstein correlations for the 158 $AGeV$ Pb+Pb collisions has not been finished yet either by the NA49 Collaboration, so that the experimental situation does not provide an definite answer yet, which one of the considered EOS gives a better description of the data.

5. Conclusions

The predominantly preliminary single and double inclusive momentum spectra of 158 $AGeV$ Pb+Pb collisions, recently measured by the NA44 and NA49 Collaborations, have been reproduced using the relativistic hydrodynamical model HYLANDER-C. However, the calculations for the much softer EOS-II yield larger slopes in many of the hadronic transverse mass spectra compared to the calculations for EOS-I. This effect is particularly strong in the transverse mass spectra of protons and anti-protons. The initial conditions, which have been found in the numerical analysis, differ strongly for the two considered scenarios. The space-time geometries in longitudinal direction and in time show a difference in the two calculations of more than a factor of 2. In contrast to the common belief [24], the Bose-Einstein correlation functions of identical pion pairs do not show such a strong, but still a significant sensitivity to the effects of the equations of state.

Acknowledgement

I would like to thank the organizers for their invitation to present these results at the "Workshop on Hydrodynamics 1997" at the ECT* in Trento/Italy. Special thanks go to D. Strottman and N. Xu for discussions that initiated this work. This work has been supported by the U.S. Department of Energy.

Notes

a. E-mail: schlei@t2.LANL.gov

b. HYLANDER-C is an improved version of the original model HYLANDER (*cf.*, refs. [10],[11],[12]).

References

1. B.R. Schlei, U. Ornik, M. Plümer, D. Strottman, R.M. Weiner, *Phys. Lett.* **B376** (1996) 212.
2. U. Ornik, M. Plümer, B.R. Schlei, D. Strottman, R.M. Weiner, *Phys. Rev.* **C54** (1996) 1381.
3. D.H. Boal, C.-K. Gelbke, B.K. Jennings, *Rev. Mod. Phys.* **62** (1990) 553.
4. R. Hanbury-Brown and R.Q. Twiss, *Philos. Mag.* **45** (1954) 663; G. Goldhaber, S. Goldhaber, W. Lee, and A. Pais, *Phys. Rev.* **120** (1960) 300.
5. Nu Xu for the NA44 Collaboration, *Nucl. Phys.* **A610** (1996) 175c.
6. I. G. Baerden et al. (NA44 Collaboration), "Midrapidity Protons in 158 *AGeV* Pb+Pb Collisions", *Phys. Lett.* **B**, (in print); CERN Preprint CERN-PPE/96-163.
7. P.G. Jones and the NA49 Collaboration, *Nucl. Phys.* **A610** (1996) 188c.
8. K. Kadija (NA49 Collaboration), *Nucl. Phys.* **A610** (1996) 248c.
9. R.B. Clare, D.D. Strottman, *Phys. Rep.* **141** (1986) 177.
10. U. Ornik, F. Pottag, R.M. Weiner, *Phys. Rev. Lett.* **63** (1989) 2641.
11. J. Bolz, U. Ornik, R.M. Weiner, *Phys. Rev.* **C46** (1992) 2047.
12. for additional detail check the web-site `http://t2.lanl.gov/schlei/hylander.html`.
13. L.D. Landau, E.M. Lifschitz, "Fluid mechanics" (Pergamon, New York, 1959).
14. F. Cooper, G. Frye, E. Schonberg, *Phys. Rev.* **D11** (1975) 192.
15. J. Bolz, U. Ornik, M. Plümer, B.R. Schlei, R.M. Weiner, *Phys. Rev.* **D47** (1993) 3860.
16. K. Redlich, H. Satz, *Phys. Rev.* **D33** (1986) 3747.
17. U. Ornik, Ph.D. thesis, Universität Marburg, 1990.
18. B.R. Schlei, Ph.D. thesis, Universität Marburg, 1994; `http://t2.lanl.gov/schlei/eprint.html`.
19. C.M. Hung, E.V. Shuryak, *Phys. Rev Lett.* **75** (1995) 4003.
20. G. Bertsch, M. Gong, and M. Tohyama, *Phys. Rev.* **C37** (1988) 1896.
21. B.R. Schlei, D. Strottman, N. Xu, "The linear correlation coefficient vs. the cross term in Bose-Einstein correlations", Los Alamos Preprint LA-UR-97-324, nucl-th/9702011, submitted to *Phys. Rev. Lett.* for publication.
22. S. Chapman, P. Scotto, U. Heinz, *Phys. Rev. Lett.* **74** (1995) 4400; *Heavy Ion Phys.* **1** (1995) 1.
23. B.R. Schlei, *Phys. Rev.* **C55** (1997) 954.
24. D.H. Rischke, *Nucl. Phys.* **A610** (1996) 88c.